Biogeochemistry **34:** 1–17, 1996.

Phosphate minerals in a lateritic crust from Venezuela

H. TIESSEN[1], S. LO MONACO[2], A. RAMIREZ[2], M. C. D. SANTOS[3] & C. SHANG[1]
[1] *Department of Soil Science, University of Saskatchewan, Saskatoon, Canada S7N 5A8;* [2] *Instituto de Ciencias de la Tierra, Facultad de Ciencias, Universidad Central de Venezuela, Caracas, Venezuela;* [3] *Departamento de Agronomia, Universidade Federal Rural de Pernambuco, Recife, Brasil*

Received 17 August 1995; accepted in revised form 9 November 1995

Key words: Carbon dating, Leucophosphite, Micromorphology, Paleo-climate, Pisolite, P-sorption

Abstract. Ferruginous crusts and pisolites have chemical and mineralogical properties that differ from the surrounding soil due to Fe and Al enrichments which cause cementations that can harden irreversibly. In addition to, and possibly as a result of the Fe and Al accumulation, other ions, particularly phosphate are often also enriched by a factor of 2–20 relative to the surrounding soil. The P accumulated in ferruginous materials is normally bound to the Fe or Al in amorphous forms of low solubility. Distinct minerals have rarely been identified.

We examined a section through a Venezuelan ferruginous crust, which contained portions with P contents >100 g kg^{-1}, chemically, mineralogically and micromorphologically with the aim to show some of the mechanisms that cause such extreme P accumulation and segregation in a landscape that is otherwise very nutrient poor.

Except for the cementation, manifested as an in-filling of pores by Fe, the morphology of the ferruginous crusts reflected that of the original soil. At approx. 30 cm below the crust's surface, goethite, strengite and leucophosphite ($KFe_2(PO_4)_2OH \cdot 2H_2O$) were identified along a downward sequence of pores nearer the surface to pores at greater depth to the matrix of the lower crust. While the lower crust contained highly soluble P, Fe oxides from outer pore spaces showed high P sorption. The element and mineral distribution across thin sections suggested that incoming Fe had interacted with a soil matrix that was exceptionally rich in K and P to form highly soluble leucophosphite, followed by less soluble strengite and finally Fe oxides that essentially occluded the more soluble minerals found in the lower crust. Associated organic C dated at 18,700 y b.p., suggesting that the occlusion process occurred around the last glacial maximum, when the region became more arid. Although extreme in its extent, the process of separation and occlusion of minerals demonstrated here, may be useful for interpreting similar processes in soils and soil cementations that affect the biogeochemical turnover of elements.

Introduction

Ferruginous crust soils are common in the semiarid and subhumid tropics where alternating moisture regimes predominate (McFarlane 1976). Ferruginous materials can occur as soft or hard nodules or gravels dispersed through soil horizons, or they can form continuous hard pans. Hard pans, because of their resistance to erosion often remain as remnants of previous episodes of soil and landscape formation, forming near-level caps on hilltops of otherwise eroded sedimentary landscapes (landscape inversion).

The high Fe (and sometimes Al) content of ferruginous materials (Anand & Gilkes 1987) imparts to them a great affinity for polyvalent anions, particularly phosphate. Therefore ferruginous gravels in contact with soil fines normally contain much greater P concentrations than the surrounding soil, and may, in addition exhibit higher P fixation capacities (Weaver et al. 1992; Tiessen et al. 1991, 1993). Ferruginous gravels in soils with 100 mg P Kg^{-1} may contain 10 to 20 times higher P concentrations than the fine soil (Tiessen et al. 1991, 1994a). No specific P minerals have been identified, and it has been assumed that ill-defined sorption products, typical for Fe-rich soils predominate. This phosphate is to a large extent present in very insoluble forms with low availability to plants or microbes, and low chemical extractability even after concretions have been ground. Although many such nodules are actively sorbing P from the surrounding soil, e.g. from fertilizer additions (Tiessen 1991), the low P content of the soils and high P content of the nodules (Tiessen 1994a) indicate that the accumulation process may possibly be ancient, dating back to nodule formation when Fe and P were supplied in drainage waters. Carbon occluded in ferruginous nodules from a top soil of the Rio Negro Basin has been dated to 4600 y in soils that otherwise contain only modern ^{14}C abundances (Tiessen et al. 1994b); occluded P probably is similarly old and inactive.

Elements occluded in boulder-sized laterite that has formed as a hard pan in a subsoil, and is now exposed as a surface crust, most certainly do not actively participate in biological or chemical transformations, and may therefore represent the product of the original formation process. We examined a portion of such a crust that showed exceptionally high P content in an otherwise nutrient-depleted landscape in eastern Venezuela, with the aim of showing some of the chemical and physical characteristics leading to element segregation in ferruginous materials.

Materials and methods

Site and sample description

The area studied is in a sub-humid savannah zone between Guasipati and Pastora in Bolivar State of Venezuela. In the region, lateritic crusts (cuirasse) are commonly encountered on top of level or nearly level hilltops at 200 m a.s.l., some 50 m above the surrounding relief. The crusts are in varying stages of physical disintegration with multiple vertical fissures and large boulders breaking off at the table margins (Figure 1). The characteristic lithology of

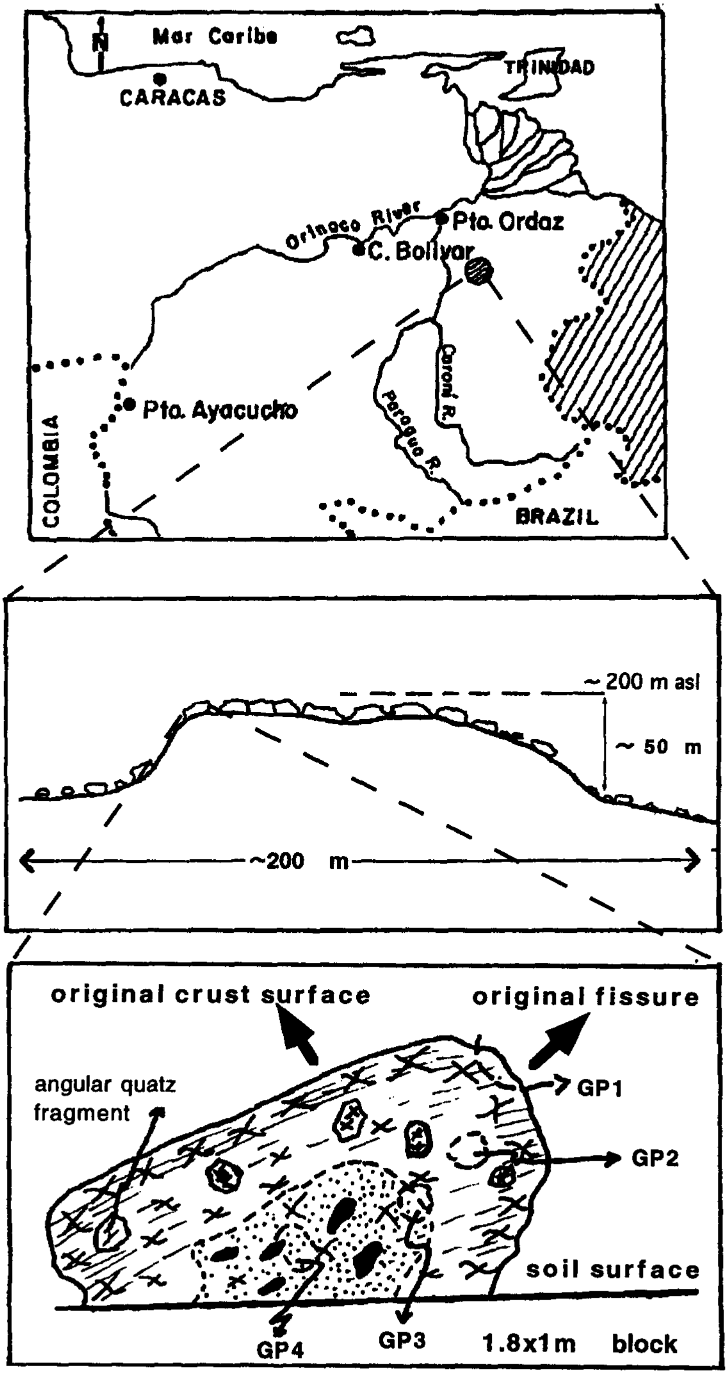

Figure 1. Sketch of sample location and position.

the area is metasediments of the proterozoic Yuruary formation (Menéndez 1968) on a basement of Guayana shield rock. The lateritic crust, of up to 1 m thickness, contains large angular and subangular quartz fragments of up to 20 cm diameter embedded in a very hard, quartzitic ferruginous mass with abundant vesicles and voids.

Samples for this study were obtained from a 1 by 1.5 m boulder which had separated from the edge of a mesa and been cut in half by earth moving equipment. Despite the disturbance, the dark weathering crust of the boulder showed that the crust was still in its original orientation. Samples of several kg each were chiselled out of the boulder and then cut with a diamond saw in the laboratory to permit sub-sampling for analysis. Samples were cut from near the surface (GP-1 and GP-2), the intermediate (GP-3), and the lower portion (GP-4) of the original crust (Figure 1), staying away from old weathered fissure surfaces, i.e. sampling from the central portion of the boulder.

Analyses

Slices were cut from sample blocks, mounted and polished into thin sections for optical and X-ray microprobe analysis. In order to investigate the element distribution in the matrix and pores of the central sample, a representative section was repeatedly scanned for the main elements Fe, Si, P and K. Output from the microprobe was captured on slides, and the element maps were digitized. The original element maps, were superimposed by the 'screen' function of Adobe Photoshop, which assigns a new pixel only to those areas that have filled pixels in both source files. It was thus possible to create maps of Fe, P and K co-occurrences.

Other analyses were performed on bulk samples of GP-1 to 4, and on specific subsamples manually scraped from sample surfaces based on appearance (Table 1). For chemical and X-ray diffraction analysis all samples were ground to 100 mesh. Elemental analysis was performed on ground samples and subsamples following the procedure of Lim & Jackson (1982): Samples were treated with conc. HNO_3 and HCl to extract Fe and Mn, followed by carbonate fusion of the residue. Aluminum, Mn and Si were determined by ICP, other metals by AAS, and Si (Jackson 1958) and P (Murphy & Riley 1962) by colorimetry. Phosphorus was extracted from ground samples by 0.01 M KCl and by anion exchange membrane (Tiessen & Moir 1993). Phosphorus sorption was determined by equilibrating 100 mg samples in 0.01 M KCl, containing between 3 and 16 mg P l^{-1} as KH_2PO_4 at pH 5.1 during three days with half an hour shaking each day. After 4 days, solution and resin extractable P were determined and P sorption calculated based on the P removed from the solution and also on the P sorbed strongly enough to remain unextractable by resin. A subsample from the central portion was analysed

Table 1. Description and main minerals of samples (≈ 5 × 5 × 5 cm blocks cut from the laterite boulder) and subsamples manually scraped out of the block surfaces.

Sample	Subsample	Description	Main component by X-ray diffract.
GP-1	1	yellow to red infill in pores	quartz, kaolinite
	2	matrix after removal of pore infill	quartz, goethite
GP-2	1	bright crystals >3 mm	pure quartz
	2	yellow to red infill in pores	quartz, kaolinite
	3	matrix after removal of pore infill	quartz, goethite
	4	Shiny black hard coating around pores	nearly pure goethite
	5	charcoaly, porous, soft in matrix	goethite
	6	hard dark brown or red grain in matrix	nearly pure goethite
GP-3	1	large bright crystals	pure quartz
	2	small (<3 mm) red granules	goethite, strengite
	3	matrix after removal of 1 & 2	goethite, strengite, quartz
GP-4	1	bright crystals	fragmented quartz
	2	yellow (>5 mm) or red (<3 mm) granules	goethite
	3	gray matrix after removal of 1 & 2	strengite, leucophosphite

for organic C by automated combustion following acid pretreatment, and a similar sample was ^{14}C dated by accelerator mass spectrometry. Inorganic C was determined by acid digestion, followed by CO_2 capture and 2-endpoint titration (Tiessen et al. 1983). Ammonia and NO_3 were extracted from the central portion with 1M KCl and analysed by Technicon auto-analysis. For X-ray diffraction, a portion of the samples was extracted with ammonium oxalate in the dark to remove amorphous oxides (Jackson et al. 1986). In some samples, a liquid magnetic separation at 0.44 Tesla was used to concentrate Fe-containing particles and reduce quartz interference (Ghabru et al. 1987). Extracted and unextracted and concentrated samples were x-rayed in the Reqacu diffractometer using Cu Kα radiation.

Results

Morphological and micromorphological description of the samples

All samples were very hard, requiring steel tools to mark the surface of sections. The surface samples GP-1 and GP-2 were similar, vesicular with several-mm large voids and consisted largely of white quartz grains in a matrix of white kaolinite and red, brown and yellow Fe-oxides. The thin section showed a large quantity of medium to fine quartz grains in a dense yellow, red and brown plasma. The only mineral in the sand and much of the silt fraction was quartz. The fine sand was predominantly rounded, but medium and coarse sand fractions were angular with low sphericity. Large grains of 1.5 to 2.0 mm were either intact of fragmented, but showed no oxide invasion in the cracks. The entire section showed an anastomosing network of channels, individual or interconnected voughs and planar voids. The plasma along pore walls was always lighter yellowish, probably due to iron migration from the matrix and different redox conditions in the pore spaces. In some of the planar voids, more recent goethite deposits were recognised by their typical optical anisotropy. Many of the channels were lined or filled with iron oxides, which accounts for the great stability of the crust (Alexander & Cady 1962). Micro-lamination of the infilling indicates that the pores were lined in several stages (Plate 1, see p. 13). The main iron oxides appeared to be goethite (yellow/brown) and hematite (blood red). X-ray microprobe analysis showed varying proportions of Fe, Al and Si across the micro-laminations.

The intermediate GP-3 and central GP-4 samples had similar appearance. Reddish-brown oxidic nodules between 2 and 20 mm diameter and angular to sub-rounded quartz fragments of up to 20 mm diameter were embedded in a yellow-white vesicular matrix. The thin section showed fewer quartz grains than were seen in the surface section, embedded in a dense ferruginous plasma of highly variable colour. The coloring of the matrix indicated the presence of goethite and other lighter brown or gray materials of finer granulometry. Pore walls were coated with a white crystalline material, similar in appearance to gibbsite. In some cases the crystals were silt size; they showed strong optical anisotropy with well-defined extinctions. Pieces of fragmented quartz grains, invaded by this light material ('runiquartz', Eswaran et al. 1975) were common in this section (Plate 2).

In general, the morphologies suggest that the upper layer had formed in the presence of greater biological activity, shown by the presence of channels, and under drier but variable conditions, shown by the lamina of red oxide deposits. The lower layer may have formed under relatively more humid conditions and with a net influx of light-coloured non-Fe-oxide materials. The abundance of this light material was responsible for the land owner bringing the site to our attention since he thought the deposit might be bauxite.

Mineralogical composition by X-ray diffraction

The relative abundance of minerals as determined by X-ray diffraction on whole samples was (Figure 2):

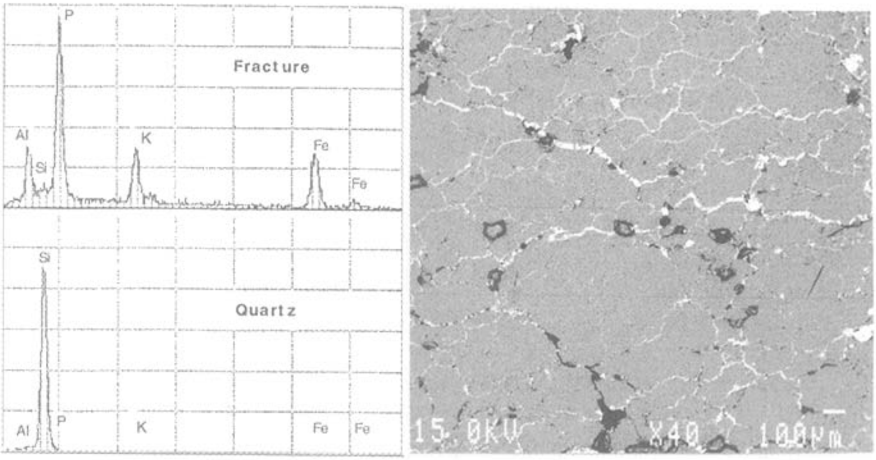

Plate 2. Back-scattered electron image of fragmented quartz from the central crust (GP4), and electron microprobe scans from areas of quartz and a fissure.

for GP-2: quartz $\geq$ goethite $\gg$ kaolinite > anatase,
for GP-3: quartz $\approx$ goethite > strengite $\gg$ anatase > phosphosiderite, and
for GP-4: quartz > leucophosphite $\geq$ strengite $\approx$ Al-substituted strengite (barrandite) $\approx$ goethite $\gg$ anatase > phosphosiderite.

Thus, X-ray diffraction, besides the expected weathering-resistant quartz, Fe-oxides and kaolinite, also showed significant amounts of phosphatic minerals in the intermediate and particularly in the lower part of the crust.

Manual separation of subsamples (Table 1) permitted a more detailed analysis: the pore-infilling of both upper crust samples was largely fine quartz, some kaolinite and minor amounts of goethite, which is responsible for the variable redness. As expected, the bright crystals were pure quartz. The main diffraction peaks of the matrix minerals were assigned to quartz and goethite. The d-spacings observed for the goethite at 0.416, 0.268 and 0.243 nm were slightly below published reference peaks (0.418, 0.269, 0.245 nm). This maybe attributable to Al substitution (Schwertman & Taylor 1989). Additional peaks at 0.256, 0.224 and 0.198 are close to those of ferrihydrite. Differently coloured yellow to red to black channel linings and grains in the matrix contained mainly quartz and goethite in varying proportions without additional differences in the X-ray diffraction pattern. Upon acid oxalate treatment a peak appeared at 0.433 nm, which might be strengite, but none of its secondary peaks were observed.

Both the matrix (3) and reddish granules (2) of the intermediate sample (GP-3) showed, in addition to the goethite and quartz peaks also observed in

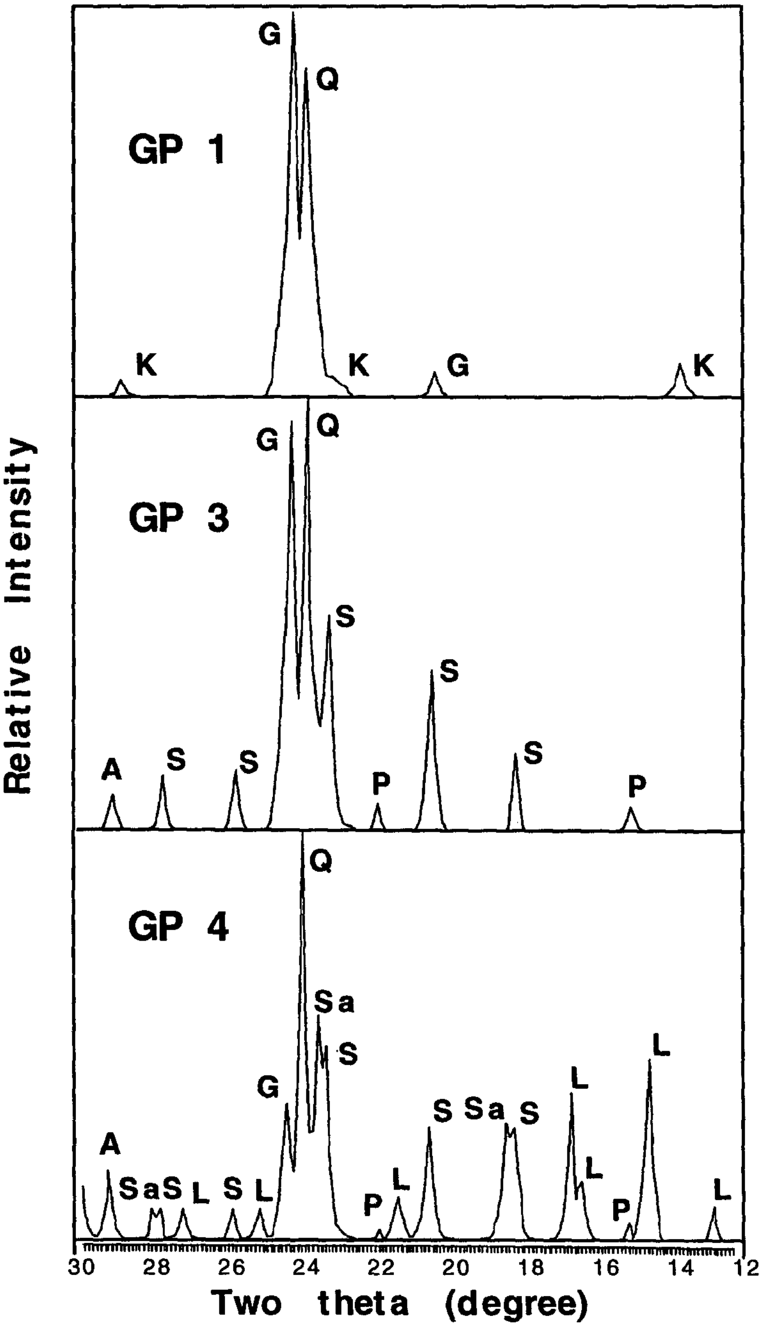

Figure 2. X-ray diffractograms of the three subsamples from: GP1-upper crust, GP3-intermediate crust, GP4-central crust. (A = anatase, G = goethite, K = kaolinite, L = leucophosphite, P = phosphosiderite, Q = quartz, S = strengite, Sa = Al-substituted strengite).

the upper crust, a sharp peak at 0.436 to 0.437 nm, and a further peak at 0.544 nm, which was enhanced in a sample concentrated by magnetic separation. This points to the presence of small amounts of strengite in these samples.

The relatively soft red-yellow granules in the central sample (GP-4, 2) were essentially goethite. It appears that with increasing oxidation towards the upper crust this material hardened, since no differences in composition were observed between the soft and hard granules. The central sample contained a number of peaks in the Fe-phosphate region (Table 2). The diagnostic peaks for leucophosphite ($KFe_2(PO_4)_2OH{\cdot}2H_2O$) were very well matched. Peaks corresponding to strengite ($FePO_4{\cdot}2H_2O$, orthorhombic) showed slightly low d-spacings, near the reference peaks for Al-substituted strengite. The matrix material (GP-4, 3) was particularly rich in phosphates. Part of the strengite signal was lost upon acid oxalate treatment. This solubility might be related to crystal imperfections from Al-substitution. The intensity of the phosphate peaks was greater in the magnetic fraction, because of the close association of P with Fe.

Elemental analyses

Iron was the main element, accounting for 17–33% of total sample weight (Table 3). The Fe content was lowest in the gray matrix of the central sample. Aluminum content ranged from 27 to 50 mg g^{-1}, increasing towards the upper crust. Manganese contents (not shown) were below 0.5 mg g^{-1} with the exception of the upper crust matrix where they reached 6 mg g^{-1}. The most striking differences across the crust were observed in P content. The P content of the upper crust was comparable with that of many other ferruginous materials in tropical soils, typically 700–800 mg kg^{-1}. The intermediate and central portions of the crust, though, contained 50 to 100 times more P, with highest concentrations in the central matrix of 111,000 mg kg^{-1} (Table 3). This explains the prominent phosphate peaks in the x-ray diffractograms, which have not been reported before for any other highly weathered soil material, such as a ferruginous crust. The central GP-4, 3 sample was the only one to contain significant amounts of K. Amounts of NH_4 (3.5 μg N g^{-1}) and NO_3 (0.2 μg N g^{-1}) extracted from the sample were negligible relative to the amount of K present, i.e. the leucophosphite had practically no NH_4 (for K) substitution. The C content of the central portion was 10.7 mg g^{-1} which is comparable to values observed in the present-day soils of the region. The presence of inorganic C could not be established; values were near the detection limit at 0.09 mg g^{-1}. The ^{14}C date of 18,700 y before present is therefore entirely attributed to organic C.

Table 2. X-ray d-spacing (nm) of the major diffraction peaks of the central (GP-4 2&3) subsamples, and reference data (relative peak intensity in parenthesis) for leucophosphite, strengite and Al-substituted strengite (Berry 1974).

GP-4, 2	GP-4, 3	Leucophosphite	Strengite	Al-strengite
0.760	0.759	0.760 (3)		
0.678	0.678	0.679 (10)		
0.598	0.597	0.599 (7)		
	0.544		0.550 (8)	0.546 (10)
0.496 (goethite)			0.495 (8)	
	0.491			0.491 (6)
0.473	0.474	0.476 (3)		
0.436	0.435		0.438 (10)	0.433 (10)
0.424 (quartz)	0.426 (quartz)			
0.416 (goethite)	0.416 (goethite)			
			0.398 (6)	0.396 (6)
0.378	0.376	0.379		
0.334 (quartz)	0.334 (quartz)			
			0.311 (8)	
	0.308			0.308 (10)
0.305	0.304	0.306 (7)		
			0.300 (6)	
	0.296			0.296 (8)
0.295	0.295		0.295 (6)	0.294 (8)
		0.292 (4)		
0.291	0.281	0.283 (4)		
	0.252		0.254 (8)	0.251 (8)

P sorption and solubility

The upper crust sample had very low soluble and resin extractable P (Table 4), together with a high P sorption of over 1000 mg kg^{-1} (Figure 3a). This is typical for ferruginous nodules and pans (Tiessen et al. 1991). Even at the highest sorption level, only 25% of the sorbed P was extractable with resin. Extractable P contents increased downward in the crust from near zero, reaching 16 mg kg^{-1} soluble P in the intermediate and 80 mg kg^{-1} in the central crust. At the same time, the goethitic granules of the intermediate zone showed a P sorption of nearly 900 mg kg^{-1} (Figure 3b) and the matrix of about 600 mg kg^{-1}, more than 60% of which was subsequently extractable with resin. In the central matrix, P sorption by the solids was only 200 mg kg^{-1}, and the high resin extractability indicated that much of this may be a very light adsorption or precipitation (Figure 3d). Particularly in the intermediate sample, high P sorption and high soluble P contents co-occurred

Table 3. Total contents of Al, Fe, Si and P of selected crust subsamples.

Element	Upper GP-2, 3	Intermediate GP-3, 2	Intermediate GP-3, 3	Central GP-4, 2	Central GP-4, 3
Al (mg g^{-1})	50.5	29.7	27.1	29.1	36.5
Al_2O_3 (%)	9.5	5.6	5.3	5.5	6.9
Fe (mg g^{-1})	319	313	211	301	171
Fe_2O_3 (%)	45.6	44.6	30.2	43.0	24.4
Si (mg g^{-1})	141	87.4	204	72.4	121
Si O_2 (%)	30.1	18.7	43.7	15.5	25.8
P (mg g^{-1})	0.825	43.8	33.7	66.4	111
PO_4 (%)	0.2	13.4	10.3	20.4	33.9
K (mg g^{-1})	<0.1	<0.1	<0.1	n.det.	36
K_2O (%)	<0.1	<0.1	<0.1	n.det.	3.0
Sum of oxides (%)	85.5	82.2	89.5	84.4	94.0

Table 4. Phosphorus extractable with KCl or resin in selected subsamples.

Subsample	0.01 M KCl extractable P mg kg^{-1}	Resin extractable P mg kg^{-1}	approx. P sorption maximum (Figure 4) mg kg^{-1}
Upper crust GP-1, 2	<0.01	2.7	1000
Intermediate GP-3, 2	16	510	900
Intermediate GP-3, 3	15	380	600
Central GP-4, 2	50	550	–
Central GP-4, 3	82	540	200

in close proximity. This may explain why the analysis of subsample GP-3, 2 yielded a relatively low soluble P of 16 mg kg^{-1}, but an extremely high resin extractable P over 500 mg kg^{-1} (Table 4): when the sample was ground and mixed, P was released from the P minerals and sorbed by the Fe-oxides, reducing the soluble P, but still maintaining a large resin P pool. Clearly the natural structure of the sample must maintain P and Fe minerals in a state far from the equilibrium that drives P minerals to dissolution and Fe minerals to sorption when the sample is ground and suspended in water or KCl. The mechanism for this separation of P and Fe species is likely to be related to sample structure, and was investigated using x-ray microprobe analysis.

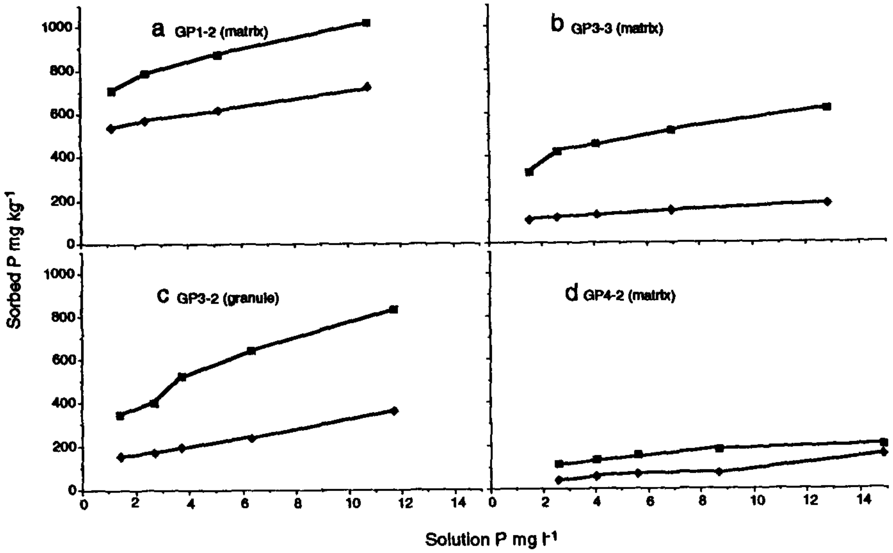

Figure 3. Phosphorus sorption of different subsamples. The lower points represent sorbed phosphate held against a subsequent resin extraction.

X-ray microprobe analysis of the central sample

In a one-point microprobe analysis, the infill in fissures of the runiquartz (Plate 2) showed strong P, K, Fe and Al peaks, consistent with the presence of leucophosphite. The P minerals in the fissures can essentially be considered as occluded by the quartz.

Element maps for Fe, Si, P and K were acquired for sections of the central portion, registered and overlaid using pixel screening (if-and logic) as required (Plate 3). Plate 3a shows the backscattered electron image from the x-ray-microprobe. The matrix and quartz is dark and the filled pores appear light. The element maps (Plate 3b, c, d) show abundant P and K in the matrix; P, K and Fe lining the pores; P and Fe filling the pore volumes;

Plate 1. Light micrograph of a thin section from the upper crust (GP1), showing microlamination of iron oxides filling pores, surrounded by fine sand-sized comminuted quatz (plane-polarised light, field width is 0.5 cm).

Plate 3. Back-scattered electron image (3a) of matrix and channels from the central crust (GP4), and elemental maps (3b = P, 3c = K, 3d = Fe) from the same area, obtained by electron microprobe scans. 3e is a composite of b, c and d and a map of Si: blue pixels show the spatial coincidence of P and K, red pixels that of P and Fe, darker purple ones that of P, K and Fe; grey areas show Si.

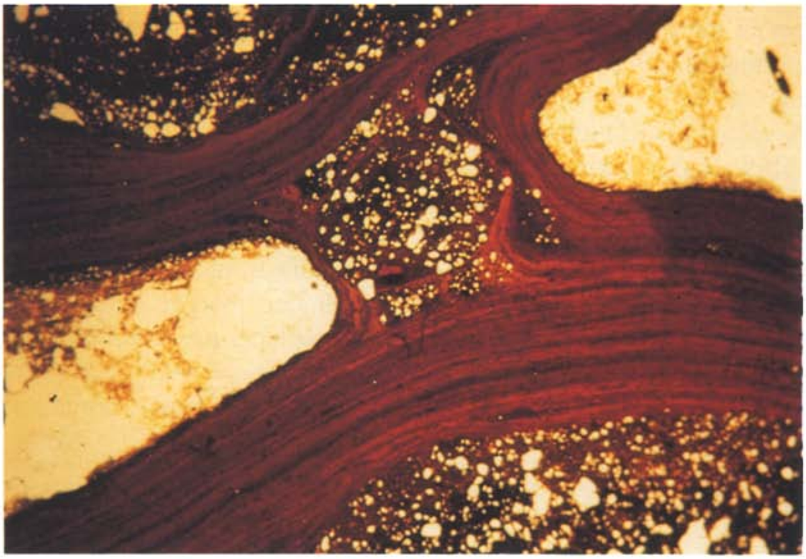

Plate 1

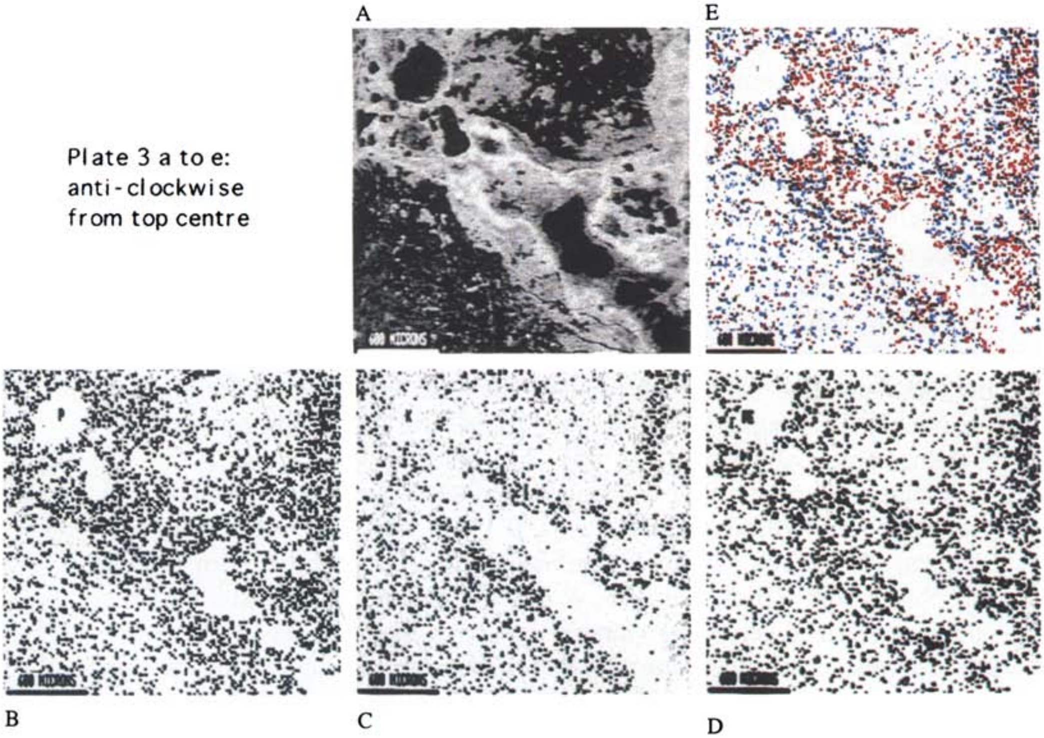

Plate 3 a to e:
anti-clockwise
from top centre

and Fe cementing the remaining voids. Potassium was most enriched along the pore margins, and was practically absent from the central pore spaces. Superimposing the original element maps by a 'screen' function produced a map of Fe, P and K interactions (Plate 3e). The blue pixels correspond to P-K spatial associations and the red ones to P-Fe associations. Dark purple or black in the mixing zone of blue and red show co-occurrence of Fe, P and K. In addition, Si was mapped with a grey inlay to distinguish quartz grains from other dark areas. These interaction maps indicate that a transition exists from K-P to K-P-Fe to P-Fe associations from the matrix to the outer pores. The leucophosphite distribution along pore margins and in some areas of the matrix can be inferred, while Fe-phosphates are enriched along pore margins and in pores. Microprobe mapping, thus, showed clear differential distributions of the main elements involved in Fe-phosphate formation in this laterite.

Discussion

There are a number of reports on leucophosphite in the literature. Most describe it as a product of mineral alteration under guano deposits (Axelrod et al. 1956; Simmons 1964; Wilson & Bain 1976) whereby K and P from the guano interact with Fe-rich minerals to form leucophosphite and associated strengite. Figure 5b in Axelrod et al. (1956) has an appearance nearly identical to the samples we analysed, with 'a breccia of hematite in phosphite cement, and transitions from leucophosphite to strengite to iron oxides in the cementations. Typically, cavities and voughs in the parent rock are in-filled with the posphite.' Guano leachates are invariably N-rich, and the resulting leucophosphite contains significant NH_4 substitution. Where the guano is of mammalian origin, an abundance of NO_3 will cause acidification and transformation of leucophosphite (which is only stable under alkaline conditions) to strengite (Axelrod et al. 1956). Our leucophosphite samples contained practically no NH_4.

Apparently non-biogenic leucophosphite has been reported from Brazil (Lindberg 1957; Bhaskara & Adusumilli 1966) and the USA (Leavens & Simpson 1975). The genesis is attributed to the leaching of Fe or Fe-Mn phosphates with K-rich solutions. While the chemical composition of the samples described here is comparable to the non-biogenic ones in the literature, the elemental distribution observed by x-ray microprobe of the thin section suggests that P and K were present prior to the invasion with Fe during the laterization process. The presence of phosphatic material in the fissures of runiquartz indicates that at some time all elements involved in the formation of phosphates (Fe, P, K and also Al) must have been mobile in the precursor material to the present laterite.

The source of P and K enrichments in this laterite is not known. We know of no P- or K-rich geological deposits in the vicinity, and guano seems an unlikely origin because of the negligible N content. Both K and P are common on sites of human habitation and fires. The nutrient-rich 'Terra Preta Do Indio' in Amazonia has been identified as of anthropogenic origin, and perhaps the present phenomenon is similar.

The microprobe mapping allows a hypothetical sequence of events to be described for the formation of this crust: (1) The original matrix was enriched in K and P, (2) Fe moved in and preferentially filled the pores, interacting along pore margins with K and P to form leucophosphite. (3) As more Fe accumulated in the pores during the ongoing laterization process, its high affinity for P caused strengite to form, while no more of the much less stable leucophosphite was formed. The strengite 'plug' is responsible for the preservation of leucophosphite in an acid environment, where it would otherwise long have been dissolved, and for the co-existence of soluble P with P sorbing phases in the crust. (4) Beyond the central crust, there is another protective layer in the form of outer pores and the upper crust which are cemented by goethite of even lower solubility, sealing the more soluble Fe phosphates off.

This scenario suggests that the original soil or saprolite was enriched with P and K prior to or in the early stages of laterisation. It is conceivable that prior to a landscape inversion, the site was in a depression, and received high P and K loads and subsequently high Fe influxes. Similar cementations above the current relief have been observed on near-by, but much older, sandstone table mountains, where local water accumulations, consequent evaporite formation and cementation, followed by erosion of the non-cemented surroundings, left Fe-rich 'stone cups' of several m diameter on otherwise plane surfaces (Briceño & Schubert 1990).

The entire process of iron phosphate formation probably occurred in a soil rather than a parent rock, since the material contains significant amounts of organic C. Assuming that the C was occluded at the same time as the leucophosphite, the formation of the whole structure can be dated. We found a ^{14}C-age of 18,700 y b.p., and since C in tropical soil has short residence times of decades rather than centuries (Trumbore 1993; Tiessen et al. 1994b), this date is likely to represent the time of occlusion. The date coincides with the last glacial maximum (Schubert 1988). Down-wind of the site along the path of the trade winds in the Venezuelan Llanos, organic matter in Paleosols was dated to 11–12,000 y b.p. (Schubert 1989). These soils were buried by aeolian sediments during a dry period. Several indicators for climatic change throughout the region indicate a dry period around 15,000 y b.p. following the last glacial maximum (Schubert 1988). The occlusion process in the laterite examined here appears to have occurred prior to the driest period, which is consistent with the process of laterite formation occurring under conditions of changeable hydric regime during the first part of the last glaciation, which started about 25,000 y b.p.

The sample site is located on the Caroní-Aro surface (200–450 m a.s.l.). This geological surface is formed by sediments on rocks of the Guayana Shield and is characterised by bornhardts covered with pisolites, which tentatively have been attributed to an earlier planation surface (Briceño & Schubert 1990). If the results presented here indeed describe the formation of the lateritic material, it may be much younger than originally thought.

Acknowledgements

This study was supported by Canadian NSERC grant OGP 0002274 and by grant 03-322750/93 of the Consejo de Desarollo Cientifico y Humanistico of the Universidad Central de Venezuela. We thank J. O. Moir (U of S) for help with the chemical analyses, B. Gomes de Almeida (UFRPE) for preparation of the thin sections and T. Bonli for help with the microprobe scans.

References

Alexander LT & Cady JG (1962) Genesis and Hardening of Laterite in Soils. Technical Bull. No. 1282. USDA, Soil Conservation Service, Washington, DC

Anand RR & Gilkes RJ (1987) Variations in the properties of iron oxides within individual specimens of lateritic crust. Aust. J. Soil Res. 25: 287–302

Axelrod JM, Carron MK & Thayer TP (1952) Phosphate mineralization at Bomi hill and Bambuta, Liberia, west Africa. Am. Mineralogist 37: 883–909

Berry LG (1977) Selected Powder Diffraction Data for Minerals. Joint Committee on Powder Diffraction Standards, Swarthmore, PA

Bhaskara RA & Adusumilli MS (1966) Leucophosphite and barbosalite from north-east Brazil. Mineral. Mag. 35: 784–785

Briceño HO & Schubert C (1990) Geomorphology of the Gran Sabana, Guayana Shield, southeastern Venezuela. Geomorphology 3: 125–141

Eswaran H, Sys C & Souza FC (1975) Plasma infusion – A pedological process of significance in the humid tropics. An. Edaf. Agrobiol. 34: 665–674

Ghabru SK, St. Arnaud RJ & Mermut AR (1987) Liquid magnetic separation of iron-bearing minerals from sand fractions of soils. Can. J. Soil Sci. 67: 561–569

Jackson ML (1958) Soil Chemical Analysis. Prentice-Hall, Inc., Englewood Cliffs, NJ

Jackson ML, Lim CH & Zelazny LW (1986) Oxides, hydroxides and aluminosilicates. In: Klute A (Ed) Methods of Soil Analysis, Part 1 (pp 113). ASA, SSSA, Madison, WI

Leavens PB & Simpson TA (1975) Iron-manganese phosphates of the Williams pegmatites, Coosa County, Alabama. Mineral. Rec. 6: 66–73

Lim CH & Jackson ML (1982) Dissolution for total elemental analysis. In: Page AL et al. (Eds) Methods of Soil Analysis, Part 2 (pp 8–11). ASA, SSSA, Madison, WI

Lindberg ML (1957) Leucophosphite from the Sapucaia pegmatite mine. Minas Gerais, Brazil. Am. Mineralogist 42: 214–221

McFarlane MJ (1976) Laterite and Landscape. Academic Press, London

Menendez A (1968) Revision de la estratigrafía de la provincia de Pastora según el estudio de la región de Guasapati, Guayana, Venezuela. Bol. Geol. 9: 309–338

Murphy J & Riley JP (1962) A modified single solution method for the determination of phosphate in natural waters. Anal. Chim. Acta 27: 31–36

Schubert C (1988) Climatic changes during the last glacial maximum in northern South America and the Caribbean: a review. Interciencia 13: 128–137

Schubert C (1989) Paleoclima del Pleistoceno tardio en el Caribe y regiones adyacentes: Un intento de compilación. Ciencia de la tierra y del espacio (La Habana) 15–16: 40–58

Schwertmann U & Taylor RM (1989) Iron oxides. In: Dixon JB & Weed SB (Eds) Minerals in Soil Environments, 2nd edition. Soil Sci. Soc. Am., Inc., Madison, WI

Simmons GC (1964) Leucophosphite, a new occurrence in the Quadrilatero Ferrifero, Minas Gerais, Brazil. Am. Mineralogist 49: 337–386

Tiessen H & Moir JO (1993) Characterisation of available P by sequential extraction. Chapter 10. In: Carter MR (Ed) Soil Sampling and Methods of Analysis (pp 75–86). Lewis Publ. CRC Press

Tiessen H, Chacon P & Cuevas E (1994a) Phosphorus and nitrogen status in soils and vegetation along a toposequence of dystrophic rainforests on the upper Rio Negro. Oecologia 99: 145–150

Tiessen H, Cuevas E & Chacon P (1994b) The role of soil organic matter in sustaining soil fertility. Nature 371: 783–785

Tiessen H, Roberts TL & Stewart JWB (1983) Carbonate analysis in soils and minerals by acid digestion and two-endpoint titration. Communications in Soil Science and Plant Analysis 14: 161–166

Tiessen H, Abekoe MK, Salcedo IH & Owusu-Bennoah E (1993) Reversibility of phosphorus sorption by ferruginous nodules. Plant and Soil 153: 113–124

Tiessen H, Frossard E, Mermut AR & Nyamekye AL (1991) Phosphorus sorption, and properties of ferruginous nodules from semiarid soils from Ghana and Brazil. Geoderma 48: 373–390

Trumbore SE (1993) Comparison of carbon dynamics in tropical and temperate soils using radiocarbon measurements. Global Biogeochemical Cycles 7: 275–290

Weaver DM, Ritchie GSP & Gilkes RJ (1992) Phosphorus sorption by gravels in lateritic soils. Aust. J. Soil Res. 30: 319–330

Wilson MJ & Bain DC (1976) Occurrence of *leucophosphite* in a soil from Elephant Island, British Antarctic Territory. Am. Mineral. 61: 1027–1028